IJASRM International Journal of Advanced Scientific Research and Management, Volume 3 Issue3, Mar 2018.
www.ijasrm.com
ISSN 2455-6378

A Comparative Comparison of Electrochemical Behaviour of Mg, Mg-5Al, Mg-10Al, Mg-15Al and Mg-Al-Zn Alloys in Alkaline NaCl solutions.

M.M. El-Rabiei [1], G.M. Abd El-Hafez [2] and Y.M. Abd El-Alim [3]

[1,2,3] Chemistry Department, Faculty of Science, Fayoum University, Fayoum-Egypt

Abstract

This research paper presents a comparative comparison of the corrosion behavior of Mg, Mg-5Al, Mg-10Al, Mg-15Al and Mg-Al-Zn alloys in alkaline NaCl solution at different concentrations. Suitable electrochemical methods were used to evaluate the corrosion rates of the specimens after immersion and exposure to polarization in the test electrolytes. Scanning electron microscope (SEM) examination was used to support the results obtained by electrochemical measurements. The data obtained in this work shows a better corrosion resistance of the Mg-Al-Zn alloy followed by Mg-5Al alloy in alkaline environment containing chloride ion. An enhanced corrosion rates were observed with increasing the chloride ion concentrations especially for pure Mg. Impedance data are in a good agree with the polarization results.

Keywords: Mg-Al alloys; Polarization measurements; EIS; Corrosion rate; SEM.

1. Introduction

In the recent years, the need for better fuel efficiency and increased performance through light weight constructions in transport system continually places new demands on the materials used. Also more environmentally-friendly materials are desired for exhaust gases reduction. The high specific strength [1] good cast ability, high damping capacity, ease of workability, low-toxicity and high thermal and electrical conductivity [2] offer Mg and its alloys as front runners in addressing the strong current need for lightweight materials in technological and structural industries to replace the heavy counterparts such as Al and steel alloys in structural components [Kaya, Kainer& Perkguleryuz, 2013]. Hence, development and research of Mg alloys for future industrial applications have inspired a great interest [Lorimer et al 2008, Kulekci et al 2008 & Cáceres et al 2009]. Unfortunately, Mg and its based alloys show inadequate corrosion resistance when they are exposed in humid or wet atmosphere and aqueous marine environment. The poor corrosion resistance of Mg and its alloys are due to two general reasons; 1st. The barrier oxide film forming on Mg based alloys is loosen making them less stable and highly corrosive especially in environments containing severe ions like chloride; 2nd. The occurrence of internal galvanic corrosion that can be caused by both impurities and secondary phases [Gao, Huang, Sheng, Zhang & Zhang, 2009]. A large body of work has been done with the aim of enhancing the corrosion resistance of Mg through the addition of alloying elements. Mg-Al alloys have been the most common category of Mg alloys, they are mainly classified into two major groups. First one: alloys containing Al (2–10%) with minor addition of Zn and Mn. The second group are those containing various elements such as rare earths (RES), zinc, thorium and silver, with absence of aluminum, have improved elevated temperature properties compared to the alloys which contain Al as a major alloying element [Revie & Uhlig,2008]. Lunder et al. [Avenue, Lein, Lunder & Nisanisanclolu, 1989] observed an enhanced corrosion resistance with the presence of 8% Al by mass fraction. Whereas, Warner et al. [Nussbaum, Stobbs, Thorne & Warner, 1992] found that the addition of 5%Al in Mg alloys is helpful in enhancing their corrosion resistance. Although alloying of Al and Zn with Mg increases their strength the secondary phases may act as a galvanic cathode and make the AZ system venerable to accelerated corrosion rate when the volume fraction of the second phases is small [Ambat et al, 2000 & Lunder et al, 1995]. On the other hand, a continuous network is formed with the presence of larger amount of second phases which can act as an anodic barrier inhibiting the overall corrosion of the alloy. The alloying effect of Al and Zn is latively less studies with this view, the present paper aimed to investigate the corrosion behavior of the Mg-5Al, Mg-10Al, Mg-15Al and Mg-Al-Zn alloys in different alkaline NaCl solutions and compare it with the behavior of pure Mg. Conventional electrochemical techniques such as potential dynamic polarization and electrochemical impedance spectroscopy, EIS, were used. The surface morphology of the investigated alloys were examined by SEM.

2. Materials and Methods

The working electrodes were prepared from commercially Mg, Mg-5Al, Mg-10Al, Mg-15Al and Mg-Al-Zn alloys. The mass spectroscopic analysis of the investigated materials is presented in Table 1.

Table. 1: Mass-spectrometric analysis of the investigated materials (mass %).

Alloys	Mg	Al	Cu	Ni	Fe	Zn
Mg	99.9	–	0.03	0.03	0.04	....
Mg-5Al	94.9	5.0	0.03	0.03	0.04	....
Mg-10Al	89.9	10.0	0.03	0.03	0.04	....
Mg-15Al	84.9	15.0	0.03	0.03	0.04	....
Mg-A-Zn	91.9	7	0.03	0.03	0.04	1

The metallic rods were mounted in suitable glass tubes by two component epoxy resin leaving a surface area of 0.5 cm2 to contact the solution. The electrochemical cell was a three electrodes all-glass cell with a Pt.-counter electrode and a saturated calomel reference (SCE) electrode. Before each experiment, the working electrode was polished mechanically using successive grades emery papers up to 2000 grit, rubbed with a smooth polishing cloth. The electrode was washed thoroughly with triple distilled water, and transferred quickly to the electrolytic cell. The electrochemical measurements were carried out in alkaline NaCl (pH.12) solutions. The effect of chloride ion concentration was studied by the addition of various amounts of NaCl ranging from 0.05 to 0.2 M. The desired pH was adjusted by small additions of 0.2 M NaOH solution. Before each experiment, the pH of the solution was controlled by a sensitive pH meter BT-500 model (Made in Germany). The polarization experiments and electrochemical impedance spectroscopic investigations, EIS, were performed using a Volta lab 10 PGZ 100 "All-in-one" ptentiostate/galvanostate. The potential were measured against and referred to the saturated calomel electrode, SCE (0.245 V vs. NHE). All potentiodynamic polarization experiments were carried out using a scan rate of 10 mVs-1. The impedance, Z, and phase shift, Ө, were recorded in the frequency domain 0.1-105 Hz. The superimposed ac-signal was 10 mV peak to peak amplitude. To achieve reproducibility, each experiment was carried out at least twice. Details of experiment procedures are as described elsewhere [Badawy et al, 2009 & Al-Kharafi et al, 1999]. A microstructural study was conducted on the different specimens. Scanning electron microscopy, SEM, used to investigate and characterize the microstructure of the different surfaces, either polished or corroded. The surface of the specimens was examined by Using SEM Model Quanta 250 FEG, FEI Company, Netherlands; (Field Emission Gun), with accelerating voltage 30 K.V., magnification14x up to 1000000 and resolution for Gun.1 n.

3. Results and Discussion

3.1. Potentiodynamic polarization measurements.

The electrochemical behavior of Mg and Mg alloys containing Al up to (5%, 10% and 15%) and (7%Al with 1% Zn) were investigated under polarization conditions. The polarization experiments were carried out at a scan rate of 10 mV/s, the potentiodynamic polarization curves for the studied materials after reaching the steadstate potential after holding of the electrode immersion in alkaline solutions of different Cl^- concentrations (0.05 M - 0.2 M) are presented in Fig. (1) (a, b & c).

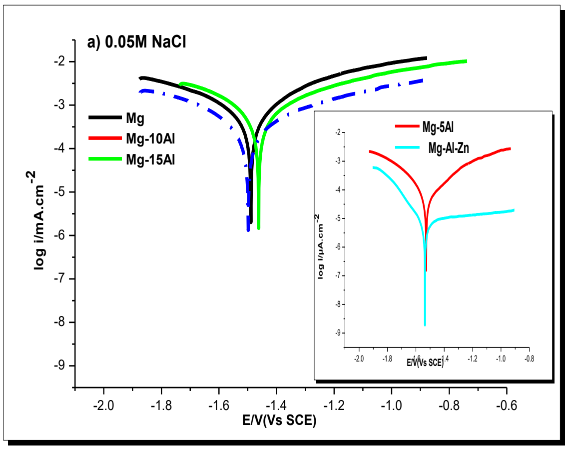

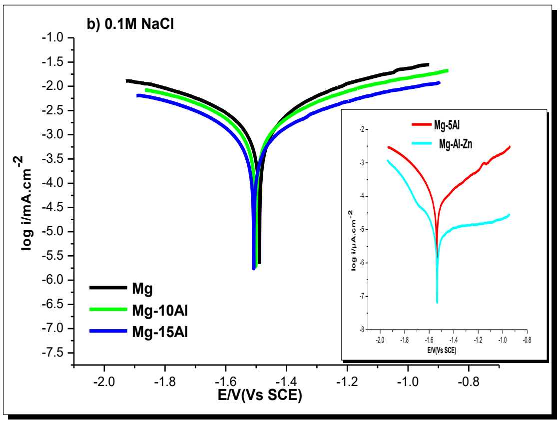

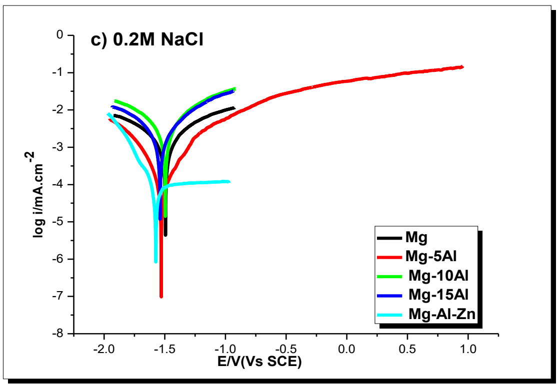

Fig.1: Potentiodynamic polarization curves for Mg and its alloys in alkaline solutions containing different Cl^- ion concentrations at 25◦C (a) 0.05 M, (b) 0.1 M and (c) 0.2 M.

As shown in Fig. (1 a, b & c), the addition of Al and Zn lead to significant shift in the polarization curves to lower current densities for all working electrodes with respect to pure Mg. Both Mg-5Al and Mg-Al-Zn alloys have the lowest corrosion current density, i_{corr}, especially in low concentrations of Cl^- ion (0.05M & 0.1M) the recorded i_{corr} was low, it was recorded in terms of (µA) as indicated from their polarization curves in Fig. (1 a&b) (present as inset), while, in the high concentration of $[Cl^-]$=0.2M, a decrease in polarization resistance and an increase in $i_{corr.}$, from µA to mA as shown in Fig. (1 c) reflecting a high corrosion rate which can be related to the participation of the Cl^- ion in the dissolution reaction through adsorption on the hydroxide barrier film covering the Mg surface transforming the $Mg(OH)_2$ to soluble $MgCl_2$ according to the following reaction [Ambat, Aung & Zhou, 2000] :

$$Mg(OH)_2 + 2Cl^- \longrightarrow MgCl_2 + 2OH^- \quad (1)$$

In chloride solutions Al_2O_3 is subjected to contentious dissolution and the corrosion prosses is taking place, the dissolution of Al [23, 24] and Al_2O_3 [25, 26] is taking place according to:

$$Al + 4Cl^- \rightarrow AlCl_4^- + 3e^- \quad (2)$$

$$4AlCl_4^- + 3H_2O \rightarrow 2Al_2O_3 + 6H^+ + 8Cl^- \quad (3)$$

$$Al^{3+} \text{ (in } Al_2O_3 \text{ n } H_2O \text{ crystalline)} + Cl^- \rightarrow Al(OH)_2Cl + 2H^+ \quad (4)$$

or

$$Al^{3+} \text{ (in } Al_2O_3\text{-n } H_2O \text{ crystalline)} + 2Cl^- \rightarrow Al(OH)_2Cl_2 + 2H^+ \quad (5)$$

The progression of these reactions results in a barrier film thinning or even breakdown in some places. An additional passivation process is taking place in Zn-containing alloys due to the formation of Zn-oxide during a dezincification process according to [Ceré, Procaccini &Vázquez, 2009]:

$$Zn + H_2O = ZnO + 2H^+ + 2e^- \quad (6)$$

The appearance of an anodic current plateau in the basic solutions suggests a passivation step [Badawy et al, 2010, Andrei et al, 2002].

From the presented data it is observed that in alkaline environment the Mg-Al-Zn and Mg-5Al alloys respectively possess the highest corrosion resistance by comparison with those containing 10 or 15% Al, this can be explained according to the potential-pH diagrams of these materials. The recorded effect of pH on the corrosion and passivation behavior of the alloy is consistent with the potential-pH diagrams of the constituent elements. Regions of stability of solid and soluble species are defined at different activities based on the data of standard free energies [Avenue, Lein, Lunder & Nisanisanclolu, 1989]. Fig. (2 a&b) shows E/pH diagrams for the elements of interest (Al and Zn) in water at 25◦C.

(a)

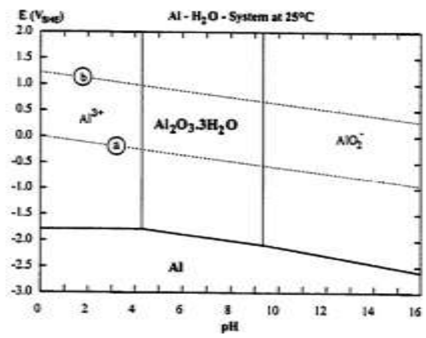

(b)

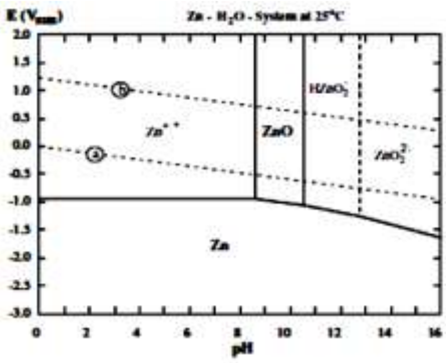

Fig. 2: Potential–pH diagrams of (a) Al and (b) Zn in aqueous solutions.

Inspection of the Pourbaix diagrams for Al and Zn implies that the Al form the most stable species in the pH range 4-9, while Zn is still active in this medium. On the other hand, Zn is passive in the range between 8.5-10.5. Hence, the Mg-Al-Zn alloy has the highest corrosion resistance in alkaline NaCl solutions compared to the investigated Mg-Al alloys. According to the investigations of Song et al. the addition of zinc affects the characteristics of the film forms on alloys surface in either binary or ternary alloys [Atrens & Song, 1999]. Also K.U. Kainer, et al. observed that Zn has improved the corrosion resistance of Mg alloys [Blawert, Dietzel, Kainer & Srinivasan, 2010].

The potentiodynamic polarization parameters, such as, corrosion potential, Ecorr, corrosion current density, i $_{corr.}$, corrosion resistance, R $_{corr}$, both Tafel slopes, the anodic, β_a, and the cathodic, β_c, and the corrosion rate were calculated and tabulated in Table (2-4).

Table 2: The Polarization parameters and rates of corrosion of Mg, Mg-5Al, Mg-10Al, Mg-15Al and Mg-Al-Z alloys in 0.05M alkaline NaCl solutions at 25 ◦C.

Alloys	E_{corr} / mV	$i_{corr.}$ mA/c m^2	R_p Ω. cm^2	β_a mv	β_c mv	Corr. Rate /mm y^{-1}
Mg	-1487.5	0.4828	94.07	242.0	-294.2	5.646
Mg-5Al	-1526.8	39.078 $\times10^{-3}$	654.87	200.1	-121.8	457.0 $\times10^{-3}$
Mg-10Al	-1461.8	0.4152	90.62	261.7	-223.9	4.856
Mg-15Al	-1498.0	0.2341	213.19	332.3	-266.0	2.737
Mg-A-Zn	-1535.6	5.6744 $\times10^{-3}$	5.63×1 03	407.5	-150.5	119.6 $\times10^{-3}$

Table 3: The Polarization parameters and rates of corrosion of Mg, Mg-5Al, Mg-10Al, Mg-15Al and Mg-Al-Z alloys in 0.1M alkaline NaCl solutions at 25 ◦C.

Alloys	E_{corr} / mV	$i_{corr\cdot}$ mA/c m2	R_p Ω. cm2	β_a mv	β_c mv	Corr. Rate /mm y-1
Mg	-1493.4	0.8075	58.31	273.2	-301.8	9.42
Mg-5Al	-1537.9	67.642 $\times10^{-3}$	564.74	355.6	-157.8	791.1 $\times10^{-3}$
Mg-10Al	-1500.8	1.0012	47.44	285.2	-283.7	11.70
Mg-15Al	-1507.5	0.4271	73.06	199.5	-180.4	4.995
Mg-Al-Zn	-1534.4	7.0858 $\times10^{-3}$	5.63 $\times10^{3}$	983.8	-133.8	210.0 ×10-3

Table 4: The Polarization parameters and rates of corrosion of Mg, Mg-5Al, Mg-10Al, Mg-15Al and Mg-Al-Z alloys in 0.2M alkaline NaCl solutions at 25 ◦C.

Alloys	E_{corr} / mV	$i_{corr\cdot}$ mA/cm2	R_p Ω. cm2	β_a mv	β_c mv	Corr. Rate /mm y-1
Mg	-1487.2	1.230	40.97	255.8	-299.2	14.38
Mg-5Al	-1528.9	0.1592	380.16	312.8	-208.6	1.86
Mg-10Al	-1495.0	1.7812	25.33	245.0	-280.8	20.83
Mg-15Al	-1538.3	1.006	35.74	223.6	-217.7	11.76
Mg-Al-Zn	-1574.0	44.9410 $\times10^{-3}$	497.25	245.7	-102.8	1.331

It clear from these results that the corrosion potential, E_{corr}, showed no specific shift with the presence of the alloying elements but the corrosion current density of pure Mg is higher than that recorded for its alloys i.e. the alloys corrosion rate is less than that of the metal itself which indicate that the presence of substituted elements (1%Zn with 7%Al and Al up to 5%) in Mg alloy showed a significant increase in the corrosion resistance in the test solutions when compared to Mg-10Al and Mg-15Al alloys. According to Warner et al. [Nussbaum, Stobbs, Thorne & Warner, 1992] the addition of 5%Al in Mg alloys is helpful in enhancing their corrosion resistance. Whereas, the addition of Al up to 8% lead to an increase of the corrosion due to the micro galvanic effect of the β-phase [31] which acts as active cathodes in the matrix.

3.2. Electrochemical impedance spectroscopic investigations.

The electrochemical impedance spectroscopy, EIS, were used to confirm the results of the potentiodynamic experiments. The experimental impedance data obtained at OCP, with pure Mg, Mg-5Al, Mg-10Al, Mg-15Al and Mg-Al-Zn alloys were recoded after 1h of the electrode immersion in alkaline NaCl solutions (0.05M-0.2M) and presented in Fig.(3 a,b&c) in the form of Nyquist plots.

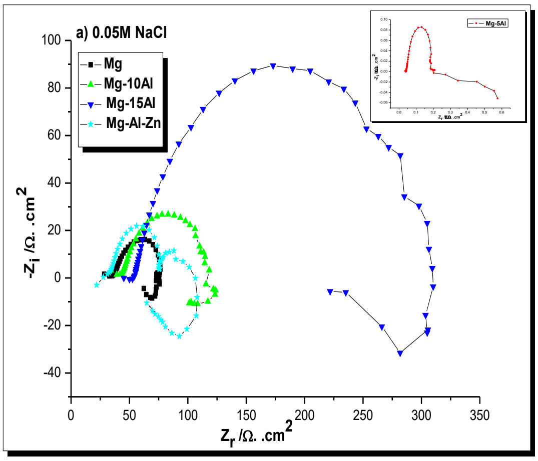

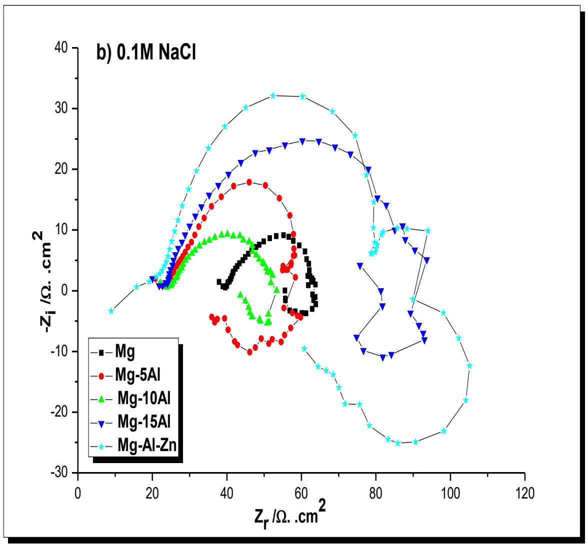

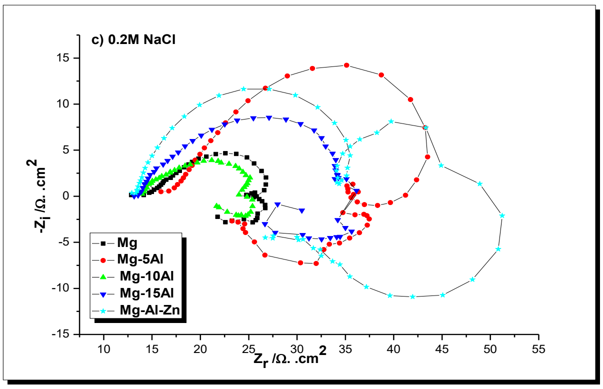

Fig. 3: Nyquist plots for Mg and different Mg-alloys in alkaline chloride solutions (a) 0.05M, (b) 0.1M and (c) 0.2M after holding at the open-circuit potential for 1h at 25^{o}c.

The response of the specimens under investigation in the Nyquist complex plane consists of one time constant except for the Mg-Al-Zn alloy the Nyquist format consists of two-time constants. In all chloride ion concentrations Mg and its binary alloys (Mg-5Al, Mg10Al and Mg-15Al) have similar impedance spectra with different diameters of the loops assigning the same corrosion mechanism of the three electrodes but with deferent corrosion rates [Bowles, Song & St John, 2004], it is worthwhile to mention that, in the dilute solution of Cl^- ion (0.05 M) the Mg- 5Al alloy has the largest arc relative to the other specimens as presented in Fig. 3a (as inset) i.e. the corrosion process taking place on this alloy surface is so limited (expressed in terms of µm/y). While the Mg-tertiary alloy (Mg-Al-Zn) show tow resistive regions (i.e. two capacitive loops) at high and low frequencies and an inductive loop at intermediate frequencies. The charge transfer resistance and the double-layer capacitance of the alloy results in the low frequency loop, while the presence of the barrier protective layer $Mg(OH)_2$ on the electrode surface caused the high frequency one. A clear increase in arc diameter was observed with the addition of (5%) Al and Zn (1%) with (7%) Al as alloying elements to Mg i.e. the presence of these elements in the α-matrix of Mg resulted in increased corrosion resistance of the metallic material. The diameter of the capacitive loops for all the studied materials deceased with the increase of the Cl^- ion concentration reflecting the enhanced corrosion rate as shown in (Fig. 3 a,b&c).

International Journal of Advanced Scientific Research and Management, Volume 3 Issue3, Mar 2018.
www.ijasrm.com
ISSN 2455-6378

The impedance data were analyzed using software provided with the impedance system where the dispersion formula was used. For a simple equivalent circuit model consisting of a parallel combination of a capacitor, C_{dl}, and a resistor, R_{ct}, in series with a resistor, R_s, representing the solution resistance. To account for the presence of a passive film, the impedance data were analyzed using the equivalent circuit model shown in Fig. 4.

(a)

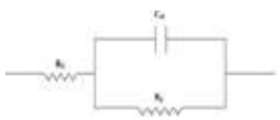

(b)

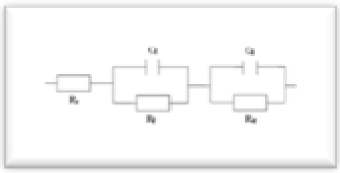

Fig. 4: Equivalent circuit model used for fitting the experimental impedance data of Mg and magnesium alloys at different conditions, R_s = solution resistance, R_{ct} = charge transfer resistance, C_{dl}= electrode capacitance, R_f = film resistance, C_f = film capacitance.
(a) Model for fitting the data of pure Mg.
(b) Model for fitting the data of Mg-5Al, Mg-10Al, Mg-15Al and Mg-Al-Zn alloys.

And another R_f C_f combination representing the passive film was introduced, where R_f, represents the film resistance and C_f, represents the barrier film capacitance. The calculated equivalent circuit parameters for the different Mg alloys in the test electrolytes are presented in Table (5-7).

Table 5: Equivalent circuit parameters for the different Mg alloys after 1h immersion in 0.05 alkaline solution at 25 ◦C.

Alloys	R_s Ω	R_{ct} Ω. Cm^2	C_{dl}/ µf. cm^{-2}	$α_1$	R_f/ Ω. Cm^2	C_f/ µf. cm^{-2}	$α_2$
Mg	36.93	49.33	5.097	1	------	------	------
Mg-5Al	48.25	179.0	4.445	0.9	------	------	------
Mg-10Al	43.63	78.96	4.031	0.9	------	------	------
Mg-15Al	54.19	254.6	6.250	0.9	------	------	------
Mg-Al-Zn	36.03	44.19	3.60	0.9	28.06	358.4	0.9

Table 6: Equivalent circuit parameters for the different Mg alloys after 1h immersion in 0.1 alkaline solution at 25 ◦C.

Alloys	R_s Ω	R_{ct} Ω. Cm^2	C_{dl}/ µf. cm^{-2}	$α_1$	R_f/ Ω. Cm^2	C_f/ µf. cm^{-2}	$α_2$
Mg	39.43	33.26	11.96	0.9	------	------	------
Mg-5Al	25.59	59.06	5.38	0.9	------	------	------
Mg-10Al	24.76	31.95	4.98	0.9	------	------	------
Mg-15Al	23.27	74.61	6.74	0.9	------	------	------
Mg-Al-Zn	24.63	65.42	3.84	0.9	11.54	551.4	0.9

Table 7: Equivalent circuit parameters for the different Mg alloys after 1h immersion in 0.2 alkaline solution at 25 ◦C.

Alloys	R_s Ω	R_{ct} Ω. Cm^2	C_{dl}/ µf. cm^{-2}	$α_1$	R_f/ Ω. Cm^2	C_f/ µf. cm^{-2}	$α_2$
Mg	15.80	13.69	14.64	0.9	------	------	------
Mg-5Al	17.58	44.72	6.53	0.9	------	------	------
Mg-10Al	13.58	16.10	9.88	0.9	------	------	------
Mg-15Al	13.46	28.69	8.76	0.9	------	------	------
Mg-Al-Zn	13.58	26.69	4.76	0.9	7.55	665.9	0.9

From the above presented data, it is obvious that the charge transfer resistance, R_{ct}, of pure Mg electrode is very small when compared to its alloys. As the Cl^- ion concentration increases a decrease in the charge transfer resistance, R_{ct}, of the different materials is observed reflecting increased corrosion rate. Hence the impedance investigations are in good agreement with the polarization measurements.

3.3. Surface Morphology Analysis.

Scanning Electron Microscopy (SEM)

SEM was carried out to study the surface morphology of the alloys under investigation, where the effect of Al and Zn on the microstructure formation and its contribution to the improvement of the corrosion resistance of the alloys can be clearly identified. Al addition to Mg as alloying element leads to the formation of the intermetallic (β phase), Fig. (5 a1-e1) presents the SE micrograph of the mechanically polished specimens.

IJASRM
International Journal of Advanced Scientific Research and Management, Volume 3 Issue3, Mar 2018.
www.ijasrm.com
ISSN 2455-6378

a1) Mg

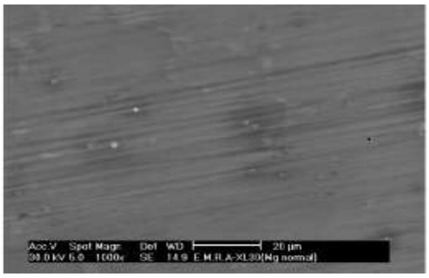

b1) Mg- 5Al

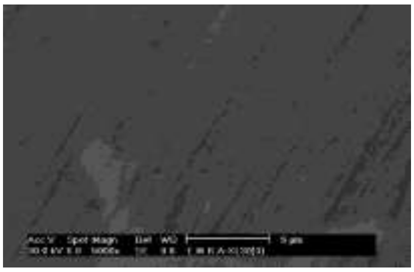

c1) Mg- 10Al

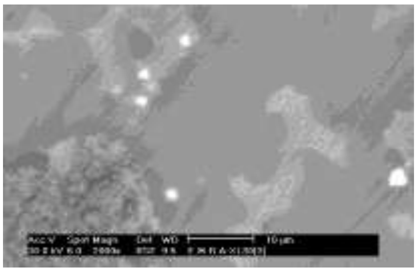

d1) Mg- 15Al

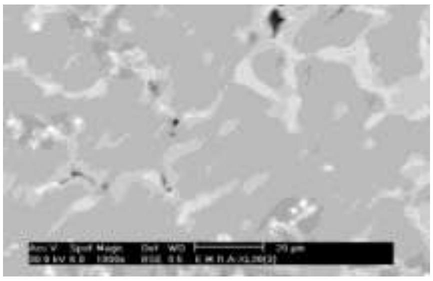

e1) Mg- Al-Zn

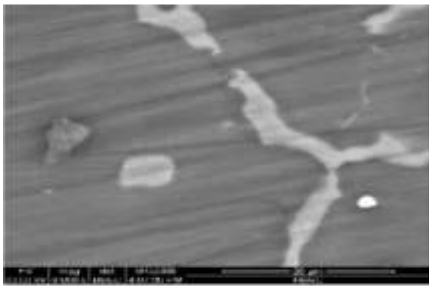

a2) Mg

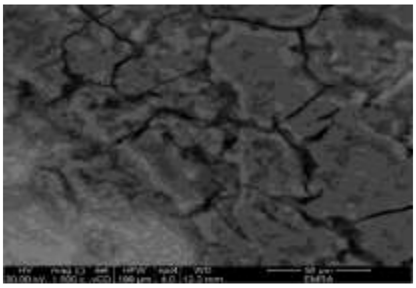

b2) Mg- 5Al

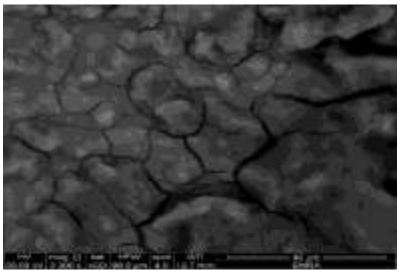

c2) Mg- 10Al

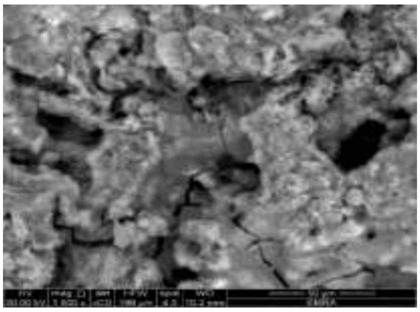

d2) Mg- 15Al

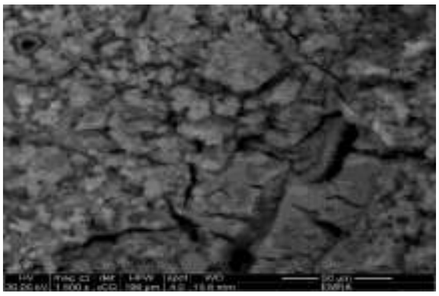

e2) Mg- Al-Zn

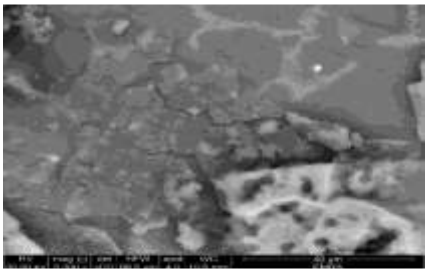

Fig. 5: SEM for the mechanically polished (a1) Mg, (b1) Mg-5Al, (c1) Mg-10Al, (d1) Mg-15Al and (e1) Mg-Al-Zn, and after immersion in alkaline 0.2M NaCl solutions for 1 h (a2) Mg, (b2) Mg-5Al, (c2) Mg-10Al, (d2) Mg-15Al and (e2) Mg-Al-Zn.

From Fig. (5 a1), it is observed that surface Mg of consists of a smooth Mg-matrix (α phase) that is easily corroded and then suppressed by the formation of the passive stable corrosion product $Mg(OH)_2$. A decreased areas of the intermetallic (β phase) can be identified on the polished surface of the Mg-5A alloy as shown in Fig. (5b1)., while, Fig. (5c1-e1) show large areas of the β phase on the surface of the other alloys.

The morphology of the studied alloys surfaces was investigated after 1 h immersion in alkaline 0.2M NaCl solutions and presented in Fig. (5 a2-e2). As seen, for all the specimens, cracked grey agglomerations of corrosion product formed on the surface and amounts of unreacted NaCl are observed. The Mg-Al alloys (%10Al, %15Al, and %5Al) respectively, shows a much more corroded surfaces rather than the Mg-Al-Zn alloy in electrolytes with the same molarity as indicated from Fig. (5 a2-e2). It can be concluded that, Mg-Al-Zn alloy is the most favorable to use in alkaline environment containing chloride ion. These results are in a good agreement with the data obtained from both potentiodynamic polarization and impedance spectroscopy.

4. Conclusions

1. The Mg-Al-Zn alloy followed by Mg-5Al alloy possessed an enhanced corrosion resistance compared to either pure Mg or its alloys those containing Al up to (10% and 15%).
2. The participation of Zn-oxide in the barrier film formed on the Mg-Al-Zn surface which is formed during a dezincification process taking place in the corrosion reaction improves the stability of this film resulting in high corrosion resistance of this magnesium alloy. Al form the most stable species in neutral solutions, while Zn is still active in this medium. Zn is passive in the range between 8.5-10.5. For this reason the corrosion resistance of Mg-Al-Zn in alkaline NaCl solutions is the greatest.
3. The specimens were proved to suffer high corrosion rates with increasing the chloride ion concentrations, a decreased diameter of the capacitive arcs resulted with high concentrations of NaCl, while large diameters were observed at low concentration.
4. SEM images have shown a suppressed effect of the intermetallic β –phase is in presence of Al up to 5%.

References

[1] Kaya A., Kainer K., Perkguleryuz M., Fundamentals of Magnesium Alloy Metallurgy, 1st ed., Woodhead, Philadelphia, (2013).
[2] Atrens A. , Song G., Corrosion Mechanisms of Magnesium Alloys, Adv. Eng. Mat. 1 (1): 11-33, (1999).
[3] Lorimer G.W., Li J.P., Robson J., Yang Z., Zhang J.X., Review on research and development of magnesium alloys, Acta Metall. Sin. 21(5): 313-328 , (2008).
[4] Kulekci M.K., Magnesium and its alloys applications in automotive industry, Int. J. Adv. Manuf. Technol. 39 (9-10): 851865, (2008).
[5] Cáceres CH. Transient environmental effects of light alloy substitutions in transport vehicles, J. Mater Design, 30 (8):.2813-2822, (2009).
[6] Gao L., Huang X., Sheng N., Zhang C., Zhang M., The corrosion of a novel Mg–11Li–3Al–0.5RE alloy in alkaline NaCl solution, J. Alloys Compd. 468 (1-2): 285-289, (2009).
[7] Revie R. W., Uhlig H. H., Corrosion and corrosion control: An Introduction to Corrosion Science and Engineering, 4th Edn. . John Wiley & Sons, Hoboken, 2008.
[8] Avenue T., Lein J.S., Lunder O., Nisanisanclolu K., Role of Mg17Al12 phase in the corrosion of Mg alloy AZ91, Corros. 45 (9): 741-748, (1989).
[9] Nussbaum G., Stobbs W.M., Thorne N. A., Warner T.J., A cross-sectional TEM study of corrosion initiation in rapidly solidified Mg-based ribbons, J. Surf. Int. Ana. 19 (1-12) 386-392 (1992).

[10] Ambat R., Aung N.N., Zhou W., Evaluation of microstructural effects on corrosion behaviour of AZ91D magnesium alloy, Corros. Sci. 42 (8): 1433-1455, (2000).
[11] Lunder O., Nisancioglu K., Videm M., Corrosion resistant magnesium alloys, SAE (1995) Transctions, Journal of Materials and Manufacturing, 104 (352-357): 950428.
[12] Badawy W.A., El-Sherif R.M. and Shehata H., Electrochemical stability of Cu–10Al–5Ni alloy in chloride–sulfate electrolytes, Electrochim. Acta 54 (19): 4501-4505, (2009).
[13] Al-Kharafi F.M., Badawy W. A., El Azab A.S., Electrochemical Behaviour and Corrosion Inhibition of Al, Al-6061 and Al-Cu in Neutral Aqueous Solutions, Corros. Sci. 41(4): 709-727, (1999).
[14] Ceré S., Procaccini R., Vázquez M., Oxygen reduction on Cu-Zn alloys, J. Appl. Electrochem. 39 (2): 177-184 (2009).
[15] Badawy W. A., El-Rabiee M., Hilal N. H., Nady H., Electrochemical behavior of Mg and some Mg alloys in aqueous solutions of different pH, Electrochimica Acta, 55 (6): 1880-1887, (2010).
[16] Andrei M., Bonora P. L., Eliezer A., Gutman E.M., Corrosion behaviour of stressed magnesium alloys, Corros. Sci. 44 (4): 729-749, (2002).
[17]Blawert C., Dietzel W., Kainer K.U., Srinivasan P.B., Corrosion of Magnesium and its Alloys, in Shreir's Corrosion, Elsevier Oxford, 3 (135): 2011-2041 (2010).
[18] Bowles A.L., Song G., St John D. H., Mater. Corrosion resistance of aged die cast magnesium alloy AZ91D Sci. Eng. A 366 (1): 74-86, (2004).